The trimer-of-hairpins motif in membrane fusion: Visna virus

Vladimir N. Malashkevich, Mona Singh*, and Peter S. Kim†

Howard Hughes Medical Institute, Whitehead Institute for Biomedical Research, Department of Biology, Massachusetts Institute of Technology, 9 Cambridge Center, Cambridge, MA 02142-1401

Contributed by Peter S. Kim, May 22, 2001

Structural studies of viral membrane fusion proteins suggest that a ''trimer-of-hairpins'' motif plays a critical role in the membrane fusion process of many enveloped viruses. In this motif, a coiled coil (formed by homotrimeric association of the N-terminal regions of the protein) is surrounded by three C-terminal regions that pack against the coiled coil in an oblique antiparallel manner. The resulting trimer-of-hairpins structure serves to bring the viral and cellular membranes together for fusion. LEARNCOIL-VMF, a computational program developed to recognize coiled coil-like regions that form the trimer-of-hairpins motif, predicts these regions in the membrane fusion protein of the Visna virus. Peptides corresponding to the computationally identified sequences were synthesized, and the soluble core of the Visna membrane fusion protein was reconstituted in solution. Its crystal structure at 1.5-Å resolution demonstrates that a trimer-of-hairpins structure is formed. Remarkably, despite less than 23% sequence identity, the ectodomains in Visna and HIV-1 envelope glycoproteins show detailed structural conservation, especially within the area of a hydrophobic pocket in the central coiled coil currently being targeted for the development of new anti-HIV drugs.

Surface glycoproteins of enveloped viruses play a critical role in viral infectivity and replication (1). These envelope proteins mediate the initial virion attachment to the cell and the subsequent fusion of the viral and cellular membranes (Fig. 1). An emerging consensus from structural studies of viral membrane fusion proteins suggests that a large number of diverse enveloped viruses use the ''trimer-of-hairpins'' motif for viral entry. In this motif, a homotrimeric coiled coil, formed by the N-terminal regions of the protein, is surrounded by three C-terminal regions that pack against the coiled coil in an oblique antiparallel manner. In a large number of known viral protein structures, including influenza hemagglutinin (2, 3), human and simian immunodeficiency virus gp41 (4–9), Moloney murine leukemia virus TM (10), Ebola virus GP2 (11, 12), human T-cell leukemia virus type 1 gp21 (13), simian parainfluenza virus 5 F1 (14), human respiratory syncytial virus F1 (15), and Newcastle disease virus F (16), the trimer-of-hairpins motif ensures that the fusion peptide (which is N-terminal of the coiled-coil domain) is spatially close to the transmembrane segment at the C terminus (Figs. 1 and 2). Given that the fusion peptide inserts into the cell membrane and the transmembrane segment is anchored in the viral membrane, formation of the trimer-of-hairpins motif is thought to facilitate the apposition of the viral and cellular membranes. But whether hairpin formation precedes the actual membrane fusion event or occurs simultaneously with fusion is unknown (see Fig. 1 legend).

In earlier work we developed a specialized program, LEARNCOIL-VMF, for identifying potential coiled coil-like regions that make up the trimer-of-hairpins motif in viral membrane fusion proteins (17). LEARNCOIL-VMF identifies such regions in a large number of viral envelope transmembrane (TM) subunits including those of many retroviruses, paramyxoviruses, and filoviruses. Notably, within the family of lentiviruses, the program found coiled coil-like regions in the Visna virus TM, which shows less than 23% sequence identity with HIV-1 gp41 (4–6). To evaluate the LEARNCOIL–VMF program and reveal whether the trimer-of-hairpins motif observed earlier in HIV-1 gp41 is indeed present in the evolutionarily distant lentivirus, we determined the crystal structure of the core of the Visna TM.

Visna, a virus that causes encephalitis, pneumonia, and arthritis in sheep, is a prototype of the family of ovine lentiviruses for which the pathogenesis and molecular biology have been characterized (18). The soluble core of the Visna TM was reconstructed by using two synthetic peptides, VN40 and VC34; these peptides were predicted by LEARNCOIL-VMF to form a trimer-of-hairpins motif (Fig. 3). In previous studies, protein dissection approaches were used to identify protease-resistant cores for viral proteins involved in membrane fusion (4, 7, 10, 12, 19, 20). In contrast, for this study the sequence analysis with LEARNCOIL-VMF was used to guide selection of the VN40 and VC34 peptides. The Visna VN40/VC34 crystal structure was solved to 1.5-Å resolution, and the resulting six-helix bundle confirmed the LEARNCOIL-VMF prediction. This structure demonstrates significant three-dimensional conservation of key features of the envelope proteins of distantly related lentiviruses despite low sequence identity between the Visna TM and HIV-1 gp41. This is especially true in the area of the prominent hydrophobic pocket that is a target for drug development against viral infection (4, 21–24).

Materials and Methods

Peptide Synthesis. The VN40 and VC34 peptides (sequences shown in Fig. 3*C*) were synthesized by using fluorenylmethoxycarbonyl peptide chemistry. Both peptides were acetylated at the N termini and amidated at the C termini. After cleavage from the resin, the peptides were desalted on a Sephadex G-25 column (Amersham Pharmacia) and lyophilized. The VN40 peptide then was dissolved in 5% acetic acid and purified by reverse-phase HPLC (Waters) with a Vydac C18 preparative column (water-acetonitrile gradient in the presence of 0.1% trifluoroacetic acid). The VC34 peptide, because of its lower solubility at low pH, was purified by using a Jupiter C18 preparative column at a pH of 6.8 (water-acetonitrile gradient in the presence of 50 mM triethylamine-acetic acid buffer). The mass of each VN40 and VC34 purified peptide was verified by matrix-assisted laser desorption ionization/time-of-flight mass spectrometry (PerSeptive Biosystems, Framingham, MA); in each case the observed mass was within 1 Da of the expected value. Both peptides were lyophilized for storage. Circular dichroism spectroscopy was performed in PBS (50 mM sodium phosphate, pH 7.0/150

Abbreviation: TM, envelope transmembrane subunit.

Data deposition: The atomic coordinates have been deposited in the Protein Data Bank, www.rcsb.org (PDB ID code 1JEK) and are available immediately at web.wi.mit.edu/kim/.

*Present address: Department of Computer Science, Lewis–Sigler Institute for Integrative Genomics, Princeton University, Princeton, NJ 08544.

†To whom reprint requests should be addressed at present address: Merck Research Laboratories, 770 Sumneytown Pike, West Point, PA 19486-0004. E-mail: peter_kim@merck.com.

The publication costs of this article were defrayed in part by page charge payment. This article must therefore be hereby marked "*advertisement*" in accordance with 18 U.S.C. §1734 solely to indicate this fact.

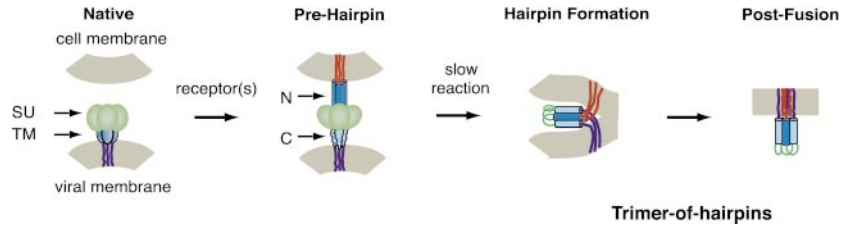

Fig. 1. Putative mechanism of membrane fusion between Visna and the host cell (adapted with modifications from ref. 21). In the native state the trimeric complex between the soluble (SU) and transmembrane subunits is formed; the fusion peptide and N-peptide (N) regions of the TM are not exposed. After interaction with the cellular receptor(s), a conformational change results in the formation of a transient prehairpin intermediate in which the fusion peptide regions (red lines) are inserted into the cell membrane, and the coiled coil of the N-peptide region of the TM (dark blue) is exposed. The C-peptide (C) region of the TM (light blue), however, is constrained and unavailable for interaction with the coiled coil. The prehairpin intermediate resolves into the trimer-of-hairpins structure, resulting in membrane fusion. The trimer-of-hairpins motif has been observed in several crystal structures of viral envelope proteins[2–15]. In this motif, the N-peptides fold into a central parallel homotrimeric coiled coil, with three C-peptides packing in an antiparallel manner along the conserved hydrophobic grooves on the coiled-coil surface. This conformation brings the fusion (red lines) and anchor (blue lines) peptides into proximity for fusion.

mM NaCl) on an AVIV Model 62DS circular dichroism spectrometer as described previously (7). Peptide concentration was determined by absorbance at 280 nm in 6 M guanidine hydrochloride (25).

Crystallization and Structure Determination. Stocks of lyophilized Visna VN40 and VC34 peptide were dissolved in water or 10 mM sodium phosphate, pH 7.5, respectively. Equimolar amounts of VN40 and VC34 were mixed, and the final protein concentration was adjusted to 10 mg/ml. After mixing, the VN40/VC34 complex demonstrated a strong tendency to aggregate. Initial crystallization conditions were found by using the vapor diffusion method with sparse matrix crystallization kits (Crystal Screen I and II, Hampton Research, Riverside, CA) and then optimized. The best diffracting crystals were produced by equilibrating 4-μl drops (protein solution mixed 1:1 with reservoir solution) for 3 months against a reservoir solution containing 25% *tert*-butanol and 0.1 M Tris-HCl, pH 8.5. The crystals belong to space group *P*321 (a = b = 52.55 Å, c = 66.75 Å; $\alpha = \beta = 90°$, $\gamma = 120°$) and contain one VN40/VC34 heterodimer in the asymmetric unit. A trimer of heterodimers is formed around the crystallographic three-fold axis. The crystals diffract beyond 1.4 Å along the crystallographic c axis but to only 1.8 Å in the orthogonal directions.

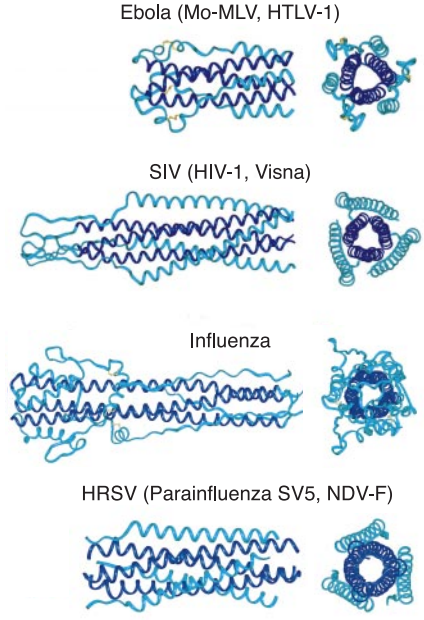

Fig. 2. Trimer-of-hairpins structures in viral membrane fusion proteins. Side and top view of fusion proteins from four different groups of viruses (only the first structure of each group is pictured): (*i*) Ebola (11, 12), Moloney murine leukemia (Mo-MLV; ref. 10), and human T-cell leukemia virus type 1 (HTLV-1; ref. 13), (*ii*) simian immunodeficiency virus (SIV; refs. 7–9), HIV-1 (4–6), and Visna (this work), (*iii*) influenza (2, 3), and (*iv*) human respiratory syncytial virus (HRSV; ref. 15), simian parainfluenza virus 5 (SV5; ref. 14), and Newcastle disease virus (NDV-F; ref. 16). The N-terminal coiled-coil cores are depicted in dark blue. In all structures, the trimer-of-hairpins conformation brings the N and C termini (right ends on the side views), and therefore the fusion peptides and transmembrane helices, into proximity for fusion. The lengths of the key elements, i.e., N helices, C helices [or in some cases extended segments (2, 3, 10–12)], and the loop regions, can vary substantially among viruses of different families. The figure was generated with INSIGHT II (31).

For data collection, crystals of Visna VN40/VC34 were harvested and flash-frozen from a drop containing reservoir solution and 20% 2-methyl-2,4-pentanediol. Diffraction data were collected at 100 K using an X-stream cryosystem and an R-AXIS IV detector (Molecular Structure, The Woodlands, TX) at the X4A beamline at the National Synchrotron Light Source (Brookhaven, NY). Diffraction intensities were integrated with DENZO and SCALEPACK software (26) and reduced to structure factors with the program TRUNCATE from the CCP4 program suite (27). The structure of Visna VN40/VC34 was solved by molecular replacement with the program AMORE (28). A polyserine model derived from the HIV-1 N36/C34 trimer (4) was used as a search model. The quality of the electron density maps (Fig. 4*D*) was significantly improved by making use of a combined maximum likelihood refinement with REFMAC and automatic water positioning with ARP (27). Model building was done with O (29), and refinement was completed with CNS (30) (Table 1).

Results

Assembling the Visna Ectodomain. Two coiled coil-like regions within the trimer-of-hairpins motif of the Visna TM (residues 688–735 and 774–804) were predicted by the LEARNCOIL-VMF program with high likelihood (>0.9; Fig. 3). Two peptides, VN40 and VC34, were synthesized on the basis of this prediction and the sequence alignment with the structure of the proteolytically stable HIV-1 N36/C34 core (4). The Visna VN40/VC34 complex was reconstituted in solution by mixing equimolar amounts of the two peptides. The complex then was crystallized, and its structure was determined by x-ray crystallography.

Crystal Structure of Visna VN40/VC34. According to the LEARNCOIL-VMF prediction, Visna VN40/VC34 forms a six-helix bundle (Fig. 4*A*) in which the VC34 helices pack in an antiparallel oblique manner against the inner coiled coil formed by the VN40

BIOCHEMISTRY

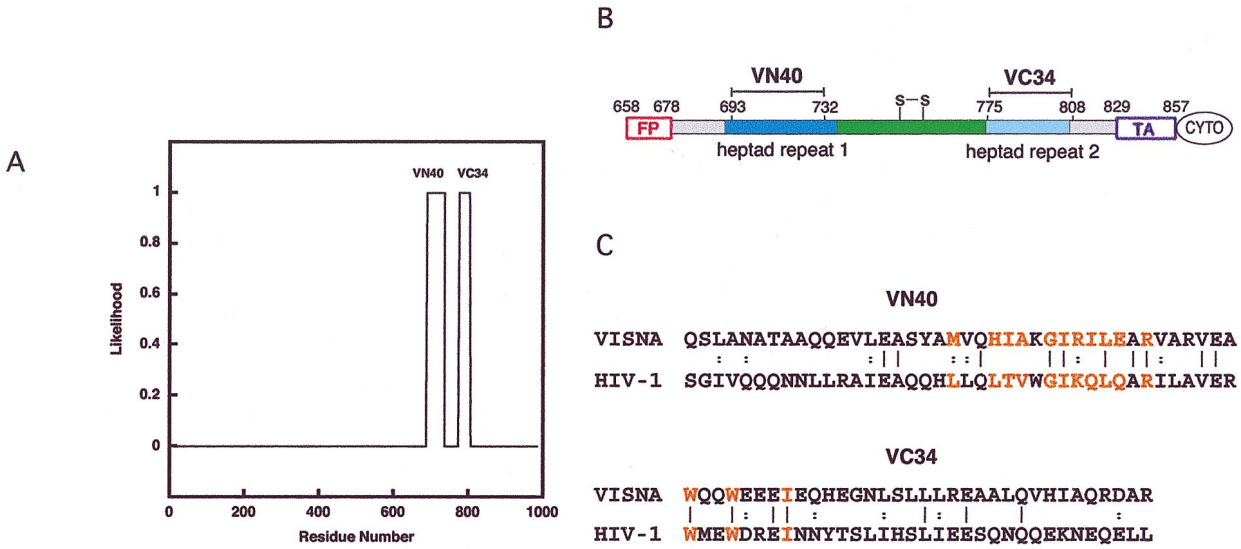

Fig. 3. Prediction of the coiled-coil domain within the Visna TM. (*A*) Two segments of the Visna TM, residues 688–735 and 774–804, are predicted by LEARNCOIL-VMF (17) with high likelihood. (*B*) A schematic view of the Visna TM showing the locations of the VN40 and VC34 peptides within the sequence. See the Fig. 1 legend for the color key. FP, fusion peptide; S-S, disulfide bond; TA, transmembrane anchor; CYTO, cytoplasmic domain. (*C*) The sequences of Visna VN40 and VC34 peptides (KV1772 strain; GenBank accession number AAA48362) and their alignment with the corresponding HIV-1 sequences (HXB2 strain; GenBank accession number K03455). Vertical bars denote identical residues, and double dots denote similar residues. Residues from N-peptides that contribute to the hydrophobic cavity and residues from the C-peptide that pack into the cavity are depicted in orange. Circular dichroism measurements indicate that VN40 and VC34 peptides are not structured in aqueous solution but form an α-helical structure when combined (V.N.M. and P.S.K., unpublished results). Thermal denaturation experiments indicate that Visna VN40/VC34 unfolds irreversibly in phosphate buffer saline, pH 7.0, with an apparent T_m of 50°C, whereas HIV-1 N36/C34 has a T_m of 68°C (see ref. 4).

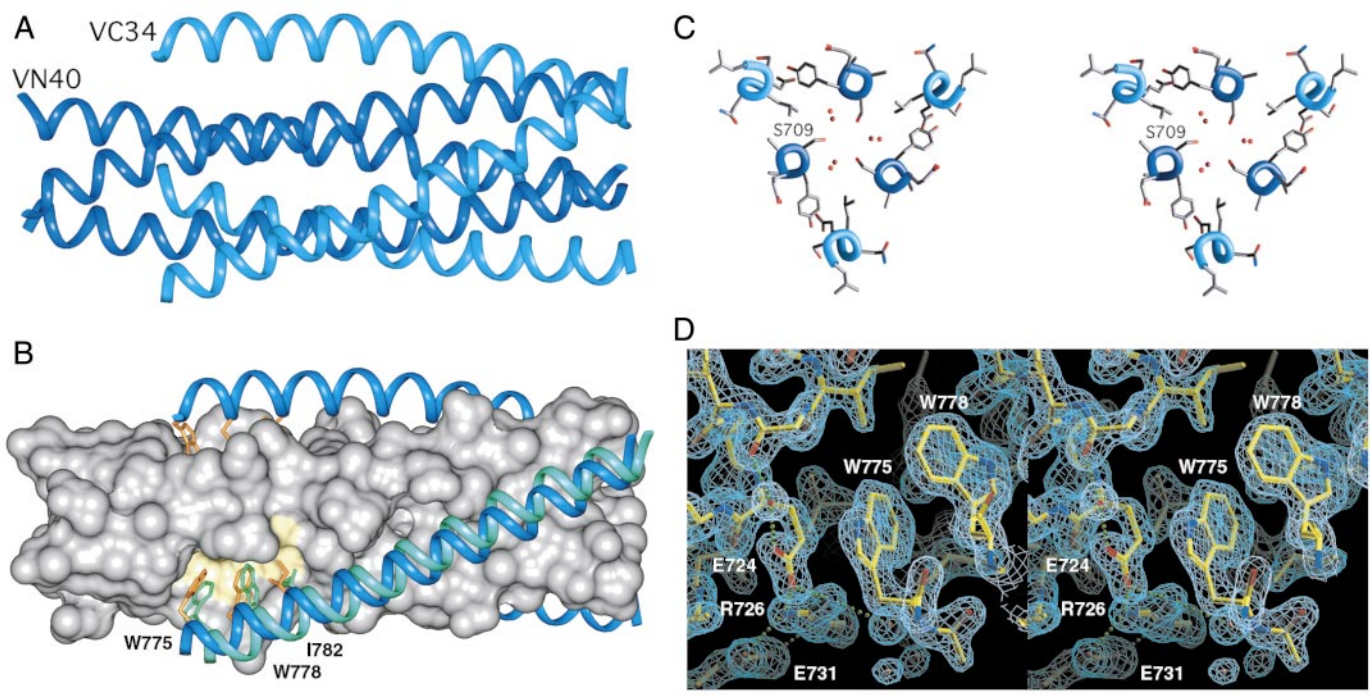

Fig. 4. Key features of the Visna VN40/VC34 structure. (*A*) Side view as shown in Fig. 2. VN40 peptides (dark blue) constitute a central coiled coil, and VC34 peptides (light blue) pack into hydrophobic grooves on the coiled-coil surface. (*B*) The location of the hydrophobic pocket (yellow) on the surface of the coiled-coil core and interactions within it are notably conserved in HIV-1 and Visna. The Visna VN40 coiled coil is represented as a molecular surface (gray), and the VC34 helices are shown as ribbons (light blue) with three side chains (orange) pointing into the hydrophobic pocket. If the N-terminal coiled-coil cores are superimposed, the C34 peptide in the HIV-1 N36/C34 structure (light green) is shifted by 2.1 Å along the groove. (*C*) Stereo view of the molecule cross-section near Ser-709. Six water molecules (red spheres) fill the void near the ring of the Ser-709 side chains grouped around the trimer axis. (*D*) Stereo view of the hydrophobic pocket area superimposed onto the final $2F_o - F_c$ electron density map. The orientation of the pocket is close to that shown in Fig. 4*B*. The C-terminal wall of the pocket (left side) is formed by the cluster of polar residues: Glu-724, Arg-726, and Glu-731. Water molecules are indicated with small red spheres. Hydrogen bonds are shown as green dotted lines. The map is contoured at 1.6σ. The figures were generated with INSIGHT II (31), GRASP (32), and O (29).

Table 1. Data collection and refinement statistics

Data collection	
Resolution, Å	20.0–1.50
Observed reflections	52,353
Unique reflections	16,300
Completeness, %	90.1 (64.7)*
R_{merge}†	0.066 (0.259)*
Refinement	
Protein nonhydrogen atoms	598
Water molecules	144
R_{cryst}‡	0.213 (0.319)*
R_{free}‡	0.265 (0.363)*
Average B-factor, Å†	31.1
RMSD from ideal geometry	
Bond length, Å	0.012
Bond angles, °	1.3
Torsion angles, °	13.9

*Values in parentheses correspond to highest resolution shell 1.52–1.50 Å.

†$R_{merge} = \Sigma\Sigma_j|I_j(hkl) - \langle I(hkl)\rangle|/\Sigma\Sigma_j|\langle I(hkl)\rangle|$, where I_j is the intensity measurement for reflection j, and $\langle I\rangle$ is the mean intensity over j reflections.

‡R_{cryst} (R_{free}) $= \Sigma||F_{obs}(hkl)| - |F_{calc}(hkl)||/\Sigma|F_{obs}(hkl)|$, where F_{obs} and F_{calc} are observed and calculated structure factors, respectively. No σ cutoff was applied. 10% of the reflections were excluded from refinement and used to calculate R_{free}.

helices. The overall structures of Visna VN40/VC34 and HIV-1 N36/VC34 are remarkably similar except for a relative 2.1-Å shift of the Visna C helices along the groove toward the C terminus of the N core and a slight decrease in the superhelical crossing angle (Fig. 4*B*). Despite the observed similarities, Visna VC34 does not form a stable heterotypic complex with HIV-1 N36 peptide (V.N.M. and P.S.K., unpublished results), whereas comparable simian immunodeficiency virus C34 peptides interact with HIV-1 N36 and inhibit HIV-1-mediated membrane fusion (7).

Asparagine, glutamine, and threonine residues are commonly observed in the nonpolar cores of viral coiled coils (2–15). Interestingly, the Visna VN40/VC34 coiled-coil core contains serine residues in position **d** of the heptad repeat. The small bulk of the serine side chains leaves a large axial void that accommodates six water molecules (Fig. 4*C*). The lack of comparably sized voids in the HIV-1 N36/C34 core might contribute to its higher thermal stability (see the Fig. 3 legend).

Hydrophobic Pocket. A prominent hydrophobic pocket very similar to the one observed in the HIV-1 gp41 structure (4, 23) is formed on the surface of the Visna VN40/VC34 coiled-coil core (Figs. 4 *B* and *D* and 5*A*). Only four of the 12 residues lining the pocket are identical in HIV-1 and Visna (Fig. 3*C*); nonetheless, the overall topology and predominantly nonpolar nature of the pocket are preserved (Fig. 5). In the Visna TM, the pocket accommodates the side chains of Trp-775, Trp-778, and Ile-782 from the C helix (equivalent to Trp-628, Trp-631, and Ile-635 of HIV-1 gp41). The C-terminal wall of the hydrophobic pocket

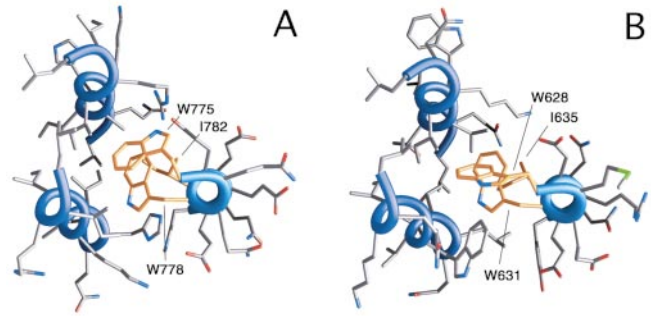

Fig. 5. Packing of the conserved hydrophobic side chains of C-peptides (orange) in the hydrophobic pockets of the Visna TM (*A*) and HIV-1 gp41 (*B*). The view along the trimer axis. Only one of three equivalent hydrophobic pockets is depicted. The figures were generated with GRASP (32).

(left half of Fig. 4 *B* and *D*) facing the indole ring of Trp-775 includes the side chains of Glu-724, Arg-726, and Glu-731, which form a hydrogen-bond network. Previous structural studies indicate that in some proteins polar side chains clustered in hydrogen-bonded networks can provide an interaction surface for nonpolar groups and rearrange easily to accommodate the binding of polar groups (33). Sequence alignments reveal that amino acid residues in the ectodomains of other lentiviruses, equivalent to Visna TM Arg-726 and Glu-731, are occupied by the oppositely charged residues, suggesting conservation of the ion pair. Remarkably, a Visna-like hydrogen-bonded side chain triplet was observed in the structure of the simian immunodeficiency virus envelope ectodomain (7–9), and the equivalent triplet (Gln-577, Arg-579, and Glu-584) is conserved among most HIV strains. Identification of the conserved polar motif within the otherwise hydrophobic pocket in HIV-1 gp41 might assist in the design of more specific small molecule inhibitors of HIV-1 fusion.

Conclusions

LEARNCOIL-VMF correctly predicts the trimer-of-hairpins motif in the Visna TM. The crystal structure of this domain is highly similar to the gp41 structure in the distantly related HIV-1, indicating structural conservation of the TM domain core within the family of lentiviruses. The two structures are notably similar within the area of the hydrophobic pocket, supporting the important role of this pocket in viral fusion and its strong potential as a target for the development of drugs that prevent viral fusion.

We thank James X. Pang for peptide synthesis and Leslie Gaffney and Alexandra Evindar for assistance in preparation of the manuscript and figures. We also thank Dr. Craig Ogata and the staff of the Howard Hughes Medical Institute beamline (X4A) at the National Synchrotron Light Source (Brookhaven National Laboratory, Brookhaven, NY) for help in data collection. This research was funded by National Institutes of Health Grant PO1 GM56552 and used the W. M. Keck Foundation X-ray Crystallography Facility at the Whitehead Institute.

1. Fields, B. N., Knipe, D. M. & Howley, P. M., eds. (1996) *Fields Virology* (Lippincott-Raven, Philadelphia), 3rd Ed.
2. Bullough, P. A., Hughson, F. M., Skehel, J. J. & Wiley, D. C. (1994) *Nature (London)* **371,** 37–43.
3. Chen, J., Lee, K.-H., Steinhauer, D. A., Stevens, D. J., Skehel, J. J. & Wiley, D. C. (1998) *Cell* **95,** 409–417.
4. Chan, D. C., Fass, D., Berger, J. M. & Kim, P. S. (1997) *Cell* **89,** 263–273.
5. Weissenhorn, W., Dessen, A., Harrison, S. C., Skehel, J. J. & Wiley, D. C. (1997) *Nature (London)* **387,** 426–430.
6. Tan, K., Liu, J., Wang, J., Shen, S. & Lu, M. (1997) *Proc. Natl. Acad. Sci. USA* **94,** 12303–12308.
7. Malashkevich, V. N., Chan, D. C., Chutkowski, C. T. & Kim, P. S. (1998) *Proc. Natl. Acad. Sci. USA* **95,** 9134–9139.
8. Caffrey, M., Cai, M., Kaufman, J., Stahl, S. J., Wingfield, P. T., Covell, D. G., Gronenborn, A. & Clore, G. M. (1998) *EMBO J.* **17,** 4572–4584.
9. Yang, Z. N., Mueser, T. C., Kaufman, J., Stahl, S. J., Wingfield, P. T. & Hyde, C. C. (1999) *J. Struct. Biol.* **126,** 131–144.
10. Fass, D., Harrison, S. C. & Kim, P. S. (1996) *Nat. Struct. Biol.* **3,** 465–469.
11. Weissenhorn, W., Carfi, A., Lee, K.-H., Skehel, J. J. & Wiley, D. C. (1998) *Mol. Cell* **2,** 605–616.
12. Malashkevich, V. N., Schneider, B. J., McNally, M. L., Milhollen, M. A., Pang, J. X. & Kim, P. S. (1999) *Proc. Natl. Acad. Sci. USA* **96,** 2662–2667.

13. Kobe, B., Center, R. J., Kemp, B. E. & Poumbouris, P. (1999) *Proc. Natl. Acad. Sci. USA* **96,** 4319–4324.
14. Baker, K. A., Dutch, R. E., Lamb, R. A. & Jardetzky, T. S. (1999) *Mol. Cell* **3,** 309–319.
15. Zhao, X., Singh, M., Malashkevich, V. N. & Kim, P. S. (2000) *Proc. Natl. Acad. Sci. USA* **97,** 14172–14177. (First Published December 5, 2000; 10.1073/pnas.260499197)
16. Chen, L., Gorman, J. J., McKimm-Breschkin, J., Lawrence, L. J., Tulloch, P. A., Smith, B. J., Colman, P. M. & Lawrence, M. C. (2001) *Structure Fold. Des.* **9,** 255–266.
17. Singh, M., Berger, B. & Kim, P. S. (1999) *J. Mol. Biol.* **290,** 1031–1041.
18. Clements, J. E. & Zink, M. C. (1996) *Clin. Microbiol. Rev.* **9,** 100–117.
19. Lu, M., Blacklow, S. C. & Kim, P. S (1995) *Nat. Struct. Biol.* **2,** 1075–1082.
20. Blacklow, S. C., Lu, M. & Kim, P. S. (1995) *Biochemistry* **34,** 14955–14962.
21. Chan, D. C. & Kim, P. S. (1998) *Cell* **93,** 681–684.
22. Ferrer, M., Kapoor, T. M., Strassmaier, T., Weissenhorn, W., Skehel, J. J., Oprian, D., Schreiber, S. L., Wiley, D. C. & Harrison, S. C. (1999) *Nat. Struct. Biol.* **6,** 953–960.
23. Eckert, D. M., Malashkevich, V. N., Hong, L. H., Carr, P. A. & Kim, P. S. (1999) *Cell* **99,** 103–115.
24. Debnath, A. K., Radigan, L. & Jiang, S. (1999) *J. Med. Chem.* **42,** 3203–3209.
25. Edelhoch, H. (1967) *Biochemistry* **6,** 1948–1954.
26. Otwinowski, Z. & Minor, W. (1997) in *Methods in Enzymology*, eds. Carter, C.W., Jr. & Sweet, R.M. (Academic, New York), Vol. 276, Part A, pp. 307–326.
27. Collaborative Computational Project, Number 4 (1994) *Acta Crystallogr. D* **50,** 760–763.
28. Navaza, J. (1994) *Acta Crystallogr. A* **50,** 157–163.
29. Jones, T. A., Zou, J. Y., Cowan, S. W. & Kjeldgaard, M. (1991) *Acta Crystallogr. A* **47,** 110–119.
30. Brünger, A. T., Adams, P. D., Clore, G. M., DeLano, W. L., Gros, P., Grosse-Kunstleve, R. W., Jiang, J.-S., Kuszewski, J., Nilges, M., Pannu, N. S., *et al.* (1998) *Acta Crystallogr. D* **54,** 905–921.
31. Molecular Simulations (1997) *Insight II, Molecular Modeling System User Guide* (San Diego).
32. Nichols, A., Sharp, K. & Honig, B. (1991) *Proteins Struct. Funct. Genet.* **11,** 281–296.
33. Malashkevich, V. N., Onuffer, J., Kirsch, J. F. & Jansonius, J. N. (1995) *Nat. Struct. Biol.* **2,** 548–553.